Comparison of ship detectability between TerraSAR-X and Sentinel-1

Domenico Velotto, Björn Tings
Department SAR Signal Processing - Maritime Safety and Security Lab
German Aerospace Center (DLR)
Bremen, Germany
{Domenico.Velotto, Bjoern.Tings}@dlr.de

Carlos Bentes
Department of Civil, Geo and Environmental Engineering
Technische Universität München (TUM)
Munich, Germany
Carlos.Bentes@tum.de

***Abstract*—In this paper, the detectability of ship signatures in Synthetic Aperture Radar (SAR) imagery acquired by the TerraSAR-X/TanDEM-X and Sentinel-1 is compared. The comparison takes into account different sensors acquisition parameters and environmental conditions on a large variety of ship size and types. In the first step, ocean targets are detected using the Near Real Time (NRT)-optimized Constant-False-Alarm-Rate (CFAR) algorithm. The optimizations include the ocean/land and false targets discrimination. In the second step, all detected targets are automatically matched in space and time with the recorded Automatic Identification System (AIS) messages. A manual cross-check is performed at the end of the assignments to have a clean SAR ship signature database. Additionally, the local wind field is retrieved from the SAR backscatter of the ocean surface surrounding the detected ships, by applying the Geophysical Model Functions (GMF) inversion XMOD2 for X-band data and CMOD5 for C-band data. Similarly, the local sea state conditions are calculated by the XWAVE and CWAVE empirical model functions. The final detectability model takes into account all SAR-based information, i.e. wind speed and sea state, as well as relevant SAR parameters, e.g. incidence angle. The overall probability of detection are derived for three ship size categories, i.e. *small*, *medium* and *large*, adopting an L2-regularized Logistic Regression classifier trained on detected and nondetected ship samples.**

Keywords—SAR, radar, target detection, ship detectability

I. INTRODUCTION

During the last decades, special interest in global maritime situation awareness has emerged, mainly due to the increasing usage of new ship routes, e.g. Artic shipping routes, and the limited coverage of coastal monitoring systems. Remotely sensed data provide a simple possibility for the monitoring of ship in open sea and not. In this sense, Synthetic Aperture Radar (SAR) data have the unique capabilities to be almost weather independent and to operate day and night [1]–[3]. Moreover, SAR is a flexible sensor able to fulfill user/application requirements with a single instrument, thanks to the possibility of implementing different operational modes.

The TerraSAR-X satellite is equipped with a X-band radar that allows a wide set of imaging modes: sub-meter Staring-Spotlight to wide coverage ScanSAR Wide. A detailed description of the TerraSAR-X Multimode SAR Processor (TMSP) with the available image products and processing level characteristics, can be found in [4]. Fig. 1 shows a composite of different TerraSAR-X imaging modes with basic characteristics given by the figure labels. For the purposes of this paper, 3 classes of image resolution are considered for TerraSAR-X products: SpotLight and Stripmap are considered *high* resolution, ScanSAR is considered *medium* resolution and ScanSAR Wide is considered *low* resolution.

With the availability of commercial Very High Resolution (VHR) X-band SAR sensors like TerraSAR-X and the Italian Cosmo-SkyMed 4 satellites constellation, the European Space Agency (ESA) Copernicus satellites, Sentinel-1A and Sentinel-1B, are SAR sensors designed to achieve medium to high resolution and wide coverage imaging capabilities. In fact, wide coverage and VHR imagery at the same time is not possible with the actual SAR system technology. The Sentinel-1 instrument payload basic information is accessible on the website [https://sentinel.esa.int/web/sentinel/missions/sentinel-1/instrument-payload]. Although the Sentinel-1 satellites offer 4 different imaging modes, only data acquired using the Interferometric Wide swath (IW) mode is considered due to the fact that this is the standard mode over European Seas [https://sentinel.esa.int/web/sentinel/missions/sentinel-

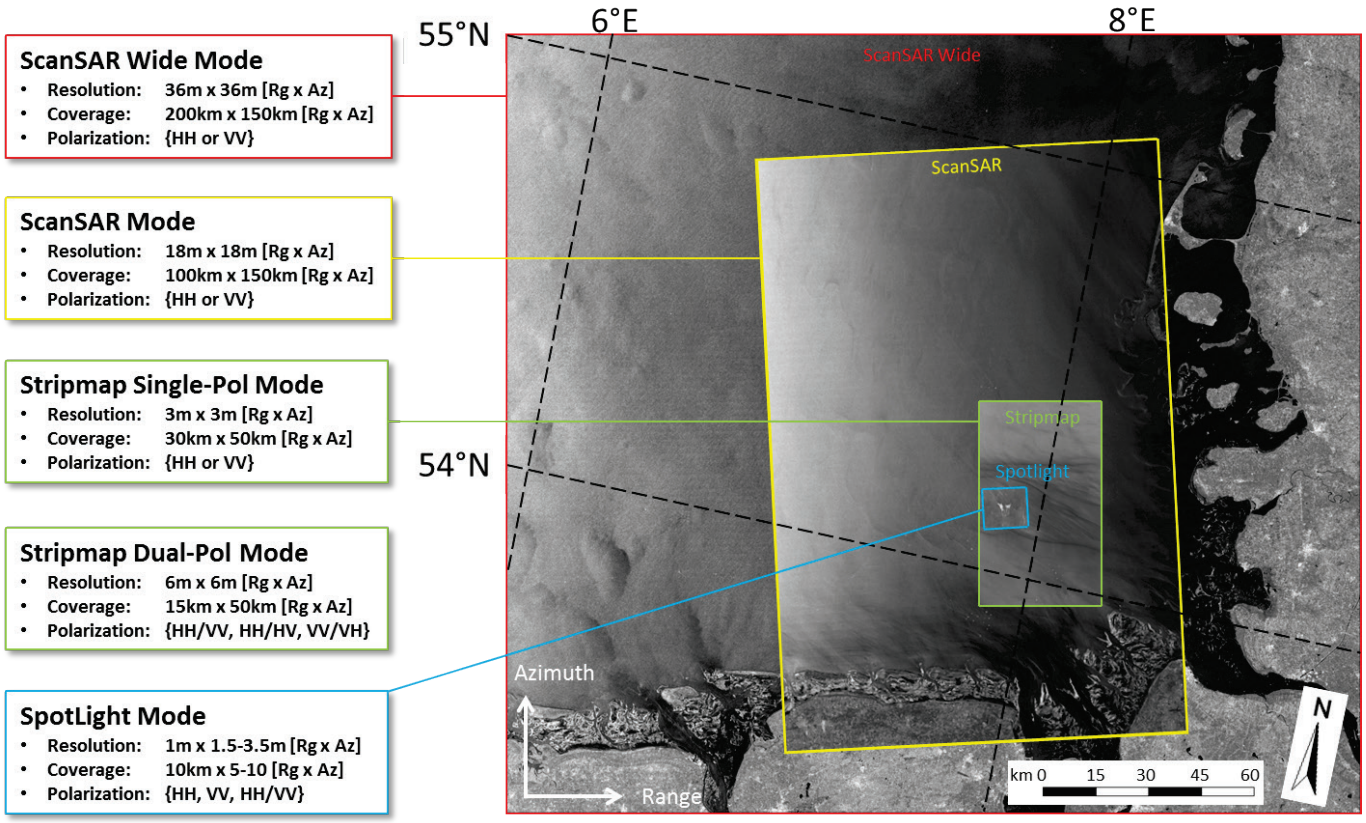

Fig. 1 Composite of different examples of TerraSAR-X imaging modes over North Sea

1/observation-scenario]. The Sentinel-1 IW Ground Range Detected (GRD) images have a geometric resolution of 20m x 22m (range x azimuth) and therefore is considered here as *medium* resolution class as comparable with the TerraSAR-X ScanSAR. Please, note that the IW mode has fixed acquisition geometry with incidence angle in near range of 29° and far range of 46°.

This paper is structured as follows: Section II gives the motivation of the work conducted; Section III summarizes the development of the data-driven detectability model and the preliminary results obtained; Section IV is dedicated to the conclusions and final remarks.

II. Motivation

Understanding the impact of different SAR imaging modes and acquisition settings on the respective information extraction methods is fundamental to estimate their performance and correctly plan future acquisitions. In order to provide a high quality Near Real Time (NRT) ship detection service, expected performances in terms of probability of detection and minimum ship size are needed. Previous studies, see [5]–[9], have approached the topic by building a prediction model which takes into account the underlying statistic of the ocean clutter radar backscatter distribution and relating the ship size to the maximum Radar Cross Section (RCS) of the ships. In this paper, a detectability model based on support vector classification is indeed proposed for both TerraSAR-X and Sentinel-1. The model takes into account: the radar incidence angle, the ship size, and the local wind speed and sea state condition. As ship size the AIS reported length has been used, while wind speed and sea state condition are directly estimated from the SAR image thanks to ad-hoc algorithms named XMOD2 [10] and XWAVE [11], [12] for X-band data and CMOD5 [13] and CWAVE [14] for C-band SAR data. With the large amount of data produced nowadays by these SAR satellites and the availability of ocean-parameters estimation algorithms, the analysis can be shifted towards a machine learning approach. Nevertheless, the simulation approach remains a valid comparison tool especially in circumstances where there is lack of data.

III. Development and Preliminary Results

The ship detectability model developed and proposed in [15] for TerraSAR-X data is here reviewed and extended to Sentinel-1 data.

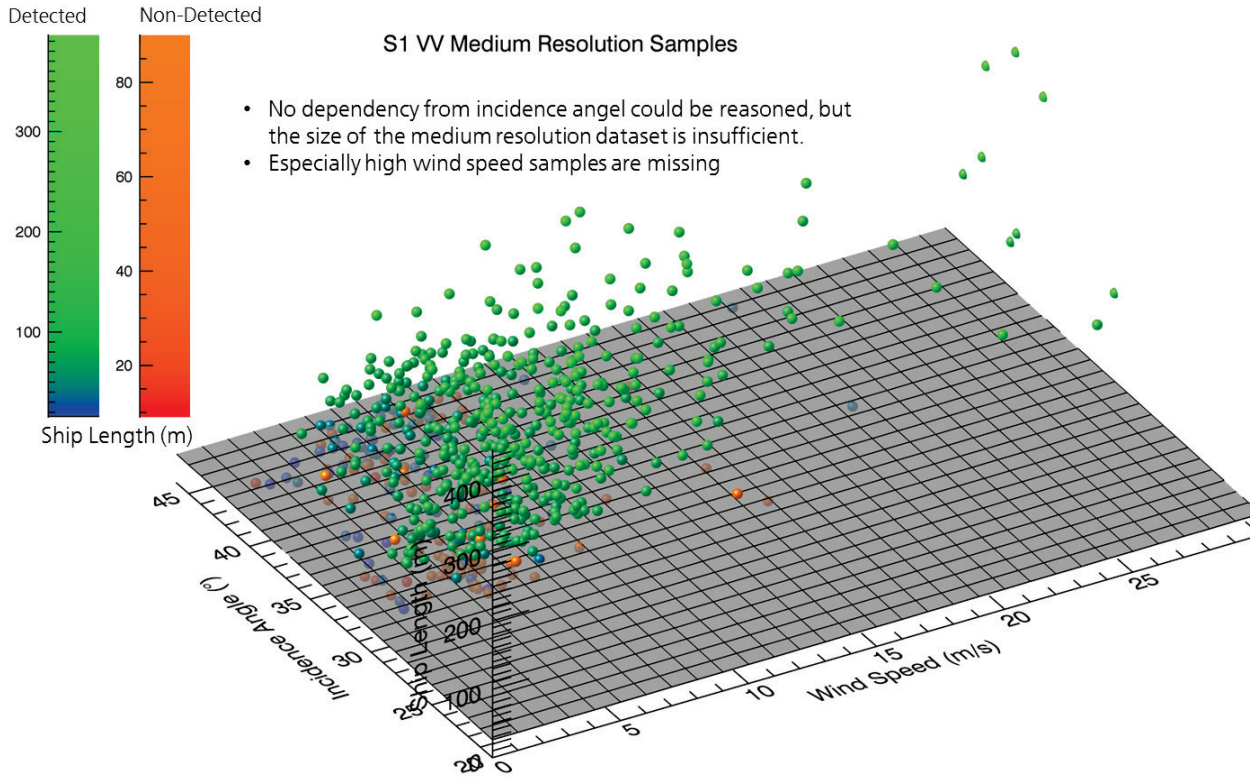

Fig. 2 Sentinel-1 medium resolution class image. Detected and nondetected ship samples are color coded in green and orange according to the ship length. The optimal linear separating hyperplane is shown in gray

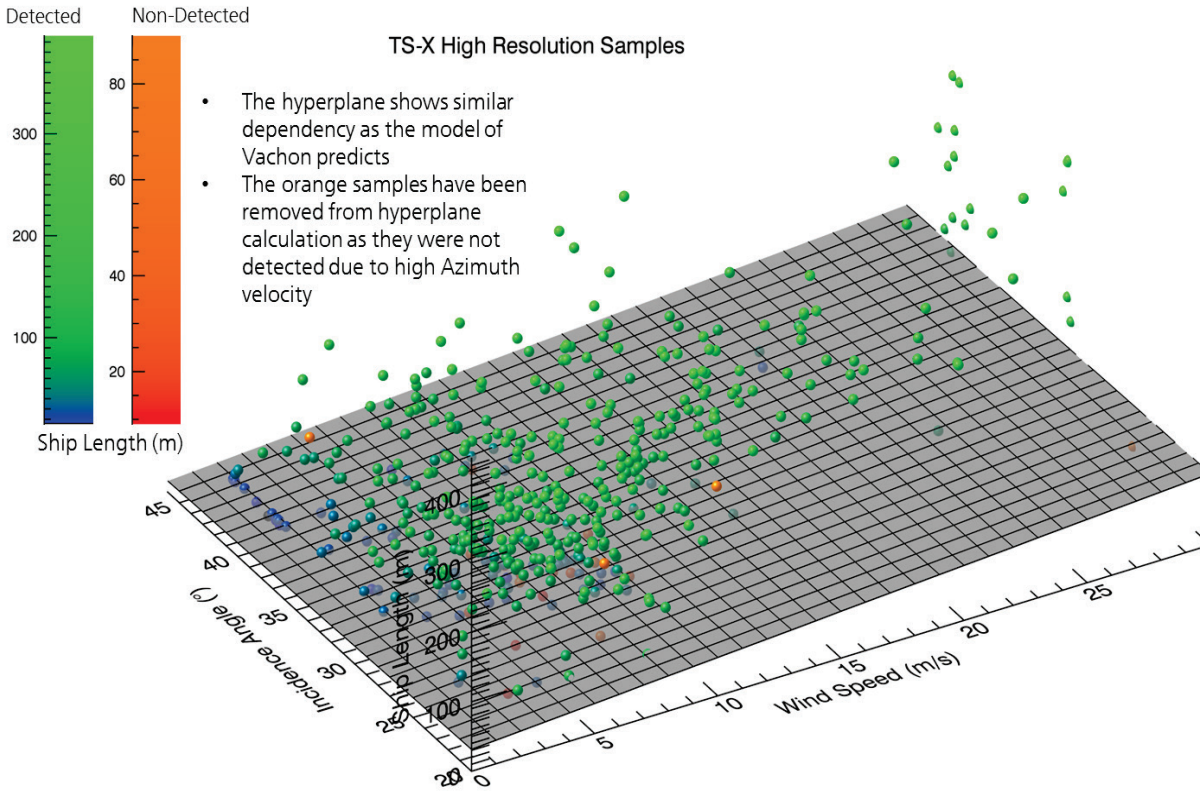

Fig. 3 TerraSAR-X high resolution class image. Detected and nondetected ship samples are color coded in green and orange according to the ship length. The optimal linear separating hyperplane is shown in gray

TABLE I. PROBABILITY OF DETECTION FOR DIFFERENT SHIP SIZE AND DATASETS

	HR TS-X	MR TS-X	LR TS-X	MR S1
Total	97%	88%	75%	88%
Small	63%	20%	9%	14%
Medium	90%	59%	27%	54%
Large	99%	99%	96%	99%

TerraSAR-X (TS-X); Sentinel-1 (S1); High- Medium- Low-Resolution (HR,MR,LR)

It is a binary classifier, with labels detected and nondetected ship, trained on the parameters ship size, incidence angle, wind speed and sea state. Please note that the sea state estimation is possible only with certain SAR image mode, e.g. TerraSAR-X Stripmap, and therefore its influence on the ship detectability model is considered only for a subset of data at hand. L2-regularized Logistic Regression classifier has been selected and the details can be found in [16], [17].

Fig. 2 and Fig. 3 illustrate the preliminary results on small datasets of high resolution TerraSAR-X and medium resolution Sentinel-1 data, where only the three parameters incidence angle, wind speed and ship length are considered. Both graphs are showing the distribution of the AIS-validated detected ship (from blue to green, depending on the ship length) and nondetected ship (from red to orange, depending on the ship length) in the two dimensional space given by wind speed and incidence angle. The optimal linear separating hyperplanes provided by L2-regularized Logistic Regression classifier can be visualized (we have not considered the sea state and therefore only three dimensions are left) and is given by the gray planes in Fig. 2 and Fig. 3. Both models confirm that the ship detectability decrease with both decreasing incidence angle and increasing wind speed. Nevertheless, this behavior is much more evident in TerraSAR-X than in Sentinel-1 where it seems that the ship detectability is not influenced by wind speed. This can be explained by the fact that the number of points available in the ranges high wind speed and low incidence angle is scarce and further data collection is currently in plan.

IV. CONCLUSIONS AND FINAL REMARKS

In this paper, the detectability of ship signatures in Synthetic Aperture Radar (SAR) imagery acquired by the TerraSAR-X/TanDEM-X and Sentinel-1 is investigated by mean of a data driven approach. The current model takes into account 3 influencing factors: 1) ship size, 2) incidence angle and 3) wind speed. The inclusion of the sea state is foreseen tighter with a larger amount of data, especially for Sentinel-1, to fill the gaps in the extreme conditions.

Table I provides the summary of the obtained probability of detection for 3 sizes of ships. Ships are grouped into three categories following the guidelines of the European Maritime Safety Agency (EMSA) for the operational ship detection services as: Small for length smaller than 15m, Medium for length between 15m and 50, and Large for length greater than 50m.

ACKNOWLEDGMENT

The author would like to thank the German Aerospace Agency (DLR) for providing the TerraSAR-X data used in this work via AO OCE3207 and the European Space Agency (ESA) for providing the Sentinel-1 data free of charge.

REFERENCES

[1] J. C. Curlander and R. N. McDonough, *Synthetic Aperture Radar: Systems and Signal Processing*. Wiley, 1991.

[2] G. Franceschetti and R. Lanari, *Synthetic Aperture Radar Processing*. CRC Press, 1999.

[3] C. Oliver and S. Quegan, *Understanding Synthetic Aperture Radar Images*. SciTech Publishing, 2004.

[4] H. Breit, T. Fritz, U. Balss, M. Lachaise, A. Niedermeier, and M. Vonavka, "TerraSAR-X SAR Processing and Products," *IEEE Trans. Geosci. Remote Sens.*, vol. 48, no. 2, pp. 727–740, Feb. 2010.

[5] P. W. Vachon, J. W. M. Campbell, C. A. Bjerkelund, F. W. Dobson, and M. T. Rey, "Ship Detection by the RADARSAT SAR: Validation of Detection Model Predictions," *Can. J. Remote Sens.*, vol. 23, no. 1, pp. 48–59, Mar. 1997.

[6] P. W. Vachon, J. Wolfe, and H. Greidanus, "Analysis of Sentinel-1 marine applications potential," in *Geoscience and Remote Sensing Symposium (IGARSS), 2012 IEEE International*, 2012, pp. 1734–1737.

[7] R. B. Olsen, T. Wahl, and G. Engen, "Expected performance of the ENVISAT ASAR for near real-time maritime applications," in *Geoscience and Remote Sensing Symposium, 1999. IGARSS '99 Proceedings. IEEE 1999 International*, 1999, vol. 2, pp. 962–964 vol.2.

[8] C. Bentes, D. Velotto, and S. Lehner, "Analysis of ship size detectability over different TerraSAR-X modes," in *Geoscience and Remote Sensing Symposium (IGARSS), 2014 IEEE International*, 2014, pp. 5137–5140.

[9] P. W. Vachon, R. English, N. Sandirasegaram, and J. Wolfe, "Development of an X-band SAR ship detectability model: Analysis of TerraSAR-X ocean imagery," Technical Memorandum DRDC Ottawa TM 2013-120, Dec. 2013.

[10] X. M. Li and S. Lehner, "Algorithm for Sea Surface Wind Retrieval From TerraSAR-X and TanDEM-X Data," *IEEE Trans. Geosci. Remote Sens.*, vol. 52, no. 5, pp. 2928–2939, May 2014.

[11] M. Bruck and S. Lehner, “Coastal wave field extraction using TerraSAR-X data,” *J. Appl. Remote Sens.*, vol. 7, no. 1, pp. 073694–073694, 2013.
[12] M. Bruck and S. Lehner, “TerraSAR-X/TanDEM-X sea state measurements using the XWAVE algorithm,” *Int. J. Remote Sens.*, vol. 36, no. 15, pp. 3890–3912, Aug. 2015.
[13] H. Hersbach, “CMOD5.N: A C-band geophysical model function for equivalent neutral wind.,” 2008. .
[14] X. M. Li, S. Lehner, and T. Bruns, “Ocean Wave Integral Parameter Measurements Using Envisat ASAR Wave Mode Data,” *IEEE Trans. Geosci. Remote Sens.*, vol. 49, no. 1, pp. 155–174, Jan. 2011.
[15] B. Tings, C. Bentes, D. Velotto, and S. Voinov, “Modelling Ship Detectability Depending On TerraSAR-X-derived Metocean Parameters,” *CEAS Space J.*, unpublished.
[16] C.-J. Lin, R. C. Weng, and S. S. Keerthi, “Trust Region Newton Methods for Large-scale Logistic Regression,” in *Proceedings of the 24th International Conference on Machine Learning*, New York, NY, USA, 2007, pp. 561–568.
[17] R.-E. Fan, K.-W. Chang, C.-J. Hsieh, X.-R. Wang, and C.-J. Lin, “LIBLINEAR: A Library for Large Linear Classification,” *J Mach Learn Res*, vol. 9, pp. 1871–1874, Jun. 2008.